

Electronic Supporting Information for

Wide-pH-range stable crystalline framework based on the largest tin-oxysulfide cluster [Sn₂₀O₁₀S₃₄]

Shan-Lin Huang,^{a,b} Liang He,^a Er-Xia Chen,^a Heng-Dong Lai,^a Jian Zhang,^{*,a} and Qipu Lin^{*,a}

^a*State Key Laboratory of Structural Chemistry Fujian Institute of Research on the Structure of Matter, Chinese Academy of Sciences, Fuzhou, Fujian 350002, China*

^b*University of Chinese Academy of Sciences, Beijing 100049, China*

*Corresponding Author: Email: zhj@fjirsm.ac.cn; linqipu@fjirsm.ac.cn

Table of Contents

Section S1: General Methods

Section S2: Synthetic Procedures

Section S3: Crystallographic Data

Section S4: Structural Pictures

Section S5: Powder X-ray Diffraction (PXRD)

Section S6: Fourier-Transform Infrared (FT-IR) Spectroscopy

Section S7: Thermostability/Chemostability

Section S8: Photoluminescence (PL)

Section S9: Photocatalytic degradation

Section S10: References

Section S1: General Methods

Chemicals: Tin tetrachloride ($\text{SnCl}_4 \cdot 5\text{H}_2\text{O}$, 99%, powder) was purchased from J&K, dimethylamine ($\text{C}_2\text{H}_7\text{N}$, 40% in water, liquid) was purchased from Aladdin, propylamine ($\text{C}_3\text{H}_7\text{N}$, $\geq 98\%$, liquid) and diethylamine ($\text{C}_4\text{H}_{11}\text{N}$, $\geq 98\%$, liquid) were purchased from Meryer, sulfur (S, 99.9%, powder), stannous chloride dihydrate ($\text{SnCl}_2 \cdot 2\text{H}_2\text{O}$, 99%, powder), ethanol ($\text{C}_2\text{H}_6\text{O}$, EtOH, 97%, liquid) and *N,N*-dimethylacetamide ($\text{C}_4\text{H}_9\text{NO}$, DMA, 97%, liquid) were purchased from Sinopharm. All chemical reagents were obtained from commercial supply without further purification.

Instrumentation: Elemental analysis (EA, with C/H/N) was carried out on a Vario EL-Cube. Powder X-ray diffraction (PXRD) patterns of the samples were recorded by a Rigaku Dmax 2500 X-ray diffractometer with Cu $K\alpha$ radiation ($\lambda = 1.54056 \text{ \AA}$). Thermal gravimetric analysis (TGA) was carried out on a Netzsch STA449F3 thermal analyzer at a temperature range of 25 to 800 °C under N_2 atmosphere with a heating rate of 10 °C min^{-1} . Fourier-transform infrared (FT-IR) spectra were recorded using a Nicolet iS10 spectrophotometer in 3750~450 cm^{-1} region. Scanning electron microscopy (SEM) and energy dispersive X-ray (EDX) spectroscopy images were obtained by a JSM-6700F. N_2 adsorption-desorption isotherms were performed on a Micromeritics ASAP 2020 surface area and pore size analyzer. Ultraviolet-visible (UV-Vis) diffuse-reflectance spectra (DRS) were performed on a Shimadzu UV-1201PC spectrophotometer. Single crystals X-ray diffraction (SCXRD) data were collected on a SuperNova diffractometer by using Cu $K\alpha$ radiation ($\lambda = 1.54178 \text{ \AA}$). The structure was solved by direct method with SHELXT program and refined by full matrix least-squares (L.S.) methods with SHELXL program of SHELX-2014 package.^[1] Mott-Schottky (MS) plots were measured on an IM 6 electrochemical system in 0.2 M Na_2SO_4 electrolyte at room temperature with Ag/AgCl electrode as the reference electrode and Pt plate as the counter electrode, at the frequencies of 1500, 2000 and 2500 Hz. Before testing, the slurry was prepared by mixing 5 mg sample with 480 μL ethanol and 20 μL Nafion, then the working electrodes were prepared by depositing 10 μL of the prepared slurry on the

surface of FTO glass plates. Photocurrent density was obtained in the presence of 0.2 M $\text{Na}_2\text{SO}_4\text{-H}_2\text{O}$ using a three-electrode cell, consisting of an F-doped SnO_2 (FTO) electrode coated with a thin layer of ground sample, a Pt-foil counter-electrode, and an Ag/AgCl reference electrode. Photocatalytic reactions were carried out in a quartz reactor with a water-cooling system. Prior to irradiation, the 3D-T4-SnOS/RhB suspension (30 mg of 3D-T4-SnOS in 50 mL of rhodamine B of $0.202 \text{ mmol L}^{-1}$) was magnetically stirred for 1 hour and then stood for 10 hours in the dark to establish the adsorption/desorption equilibrium. Then, a 300 W Xe lamp with a 420 nm cut-off filter was used as illuminating source. At a regular interval of time (0.5 hour), 1 mL of reaction solution was extracted and filtrated to remove the solid-state species. The absorbance of the filtrated solution was measured by using UV-Vis spectroscopy. After reaction, the mixture was centrifuged and the powder was collected for the PXRD testing.

Section S2: Synthetic Procedures

(1) Synthesis of 3D-T4-SnOS

S powder (60 mg, 1.88 mmol), $\text{SnCl}_2 \cdot 2\text{H}_2\text{O}$ (54 mg, 0.24 mmol), $\text{SnCl}_4 \cdot 5\text{H}_2\text{O}$ (428 mg, 1.22 mmol), propylamine ($\text{C}_3\text{H}_7\text{N}$, 3.0 mL), *N,N*-dimethylacetamide ($\text{C}_4\text{H}_9\text{NO}$, 3.0 mL) and ethanol ($\text{C}_2\text{H}_6\text{O}$, 1.0 mL) were mixed in a 23 mL teflon-lined stainless autoclave and stirred for about 30 minutes. The vessel was sealed and heated at 160 °C for 7 days. After cooling to room temperature, yellow octahedral crystals of 3D-T4-SnOS were obtained after washing with DMA and EtOH to remove precipitates, and then dried in air (ca. 42% yield based on sulfur). EA data: C 11.52, H 2.12, N 3.04, S 22.95%, calculated for $\text{C}_{48}\text{H}_{125}\text{N}_9\text{O}_{23}\text{S}_{32}\text{Sn}_{20}$ C 11.31, H 2.33, N 3.14, S 23.04%. IR: ν (cm^{-1}) = 2923 (w), 1610 (m), 1458 (w), 1395 (w), 1262 (w), 1115 (w), 1015 (w), 630 (s), 556 (w), 420 (w).

(2) Synthesis of 2D-T3-SnOS (with the same $\text{T3-Sn}_{10}\text{O}_4\text{S}_{20}$ cluster and two-dimensional network as TMA-SnOS-SB3)^[2]

S powder (110 mg, 3.44 mmol), $\text{SnCl}_4 \cdot 5\text{H}_2\text{O}$ (383 mg, 1.09 mmol), dimethylamine ($\text{C}_2\text{H}_7\text{N}$, 2.0 mL) and diethylamine ($\text{C}_4\text{H}_{11}\text{N}$, 4.0 mL) were mixed in a 23 mL teflon-lined stainless autoclave and stirred for about 30 minutes. The vessel was sealed and heated at 180 °C for 8 days. After cooling to room temperature, pale-yellow octahedral crystals of 2D-T3-SnOS were obtained after washing with EtOH to remove precipitate, and then dried in air (ca. 27% yield based on sulfur). IR: ν (cm^{-1}) = 3490 (w), 3046 (m), 2974 (m), 2762 (w), 1569 (w), 1442 (m), 1383 (w), 1053 (w), 1020 (w), 773(w), 570 (s).

Section S3: Crystallographic Data

Table S1 Crystallographic data of 3D-T4-SnOS

Compound Reference	3D-T4-SnOS
Chemical Formula	$(\text{C}_3\text{H}_8\text{N})_4[\text{Sn}_{20}\text{O}_{10}\text{S}_{32}] \cdot (\text{C}_4\text{H}_9\text{NO})_5(\text{C}_2\text{H}_6\text{O})_8$
Formula Mass	4604.35
Crystal System	Tetragonal
$a/\text{\AA}$	23.5105(5)
$b/\text{\AA}$	23.5105(5)
$c/\text{\AA}$	40.205(3)
$\alpha/^\circ$	90
$\beta/^\circ$	90
$\gamma/^\circ$	90
Unit-Cell Volume/ \AA^3	22223(2)
Temperature/K	293(2)
Space Group	$I4_1/acd$
No. of Formula Units Per Unit-Cell, Z	8
No. of Reflections Measured	20736
No. of Independent Reflections	5597
R_{int}	0.0384
Final R_1 Values ($I > 2\sigma(I)$)	0.0410
Final $wR(F^2)$ Values ($I > 2\sigma(I)$)	0.1077
Final R_1 Values (all data)	0.0539
Final $wR(F^2)$ Values (all data)	0.1173
Goodness of Fit on F^2	1.012
CCDC Number	1909342

Section S4: Structural Pictures

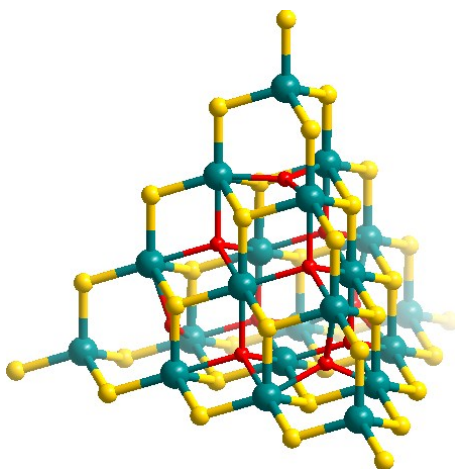


Fig. S1 Supertetrahedral filled-T4 “[$\text{Sn}_{20}\text{O}_{10}\text{S}_{34}$]” cluster with the missing of the central sulfide anion of 3D-T4-SnOS.

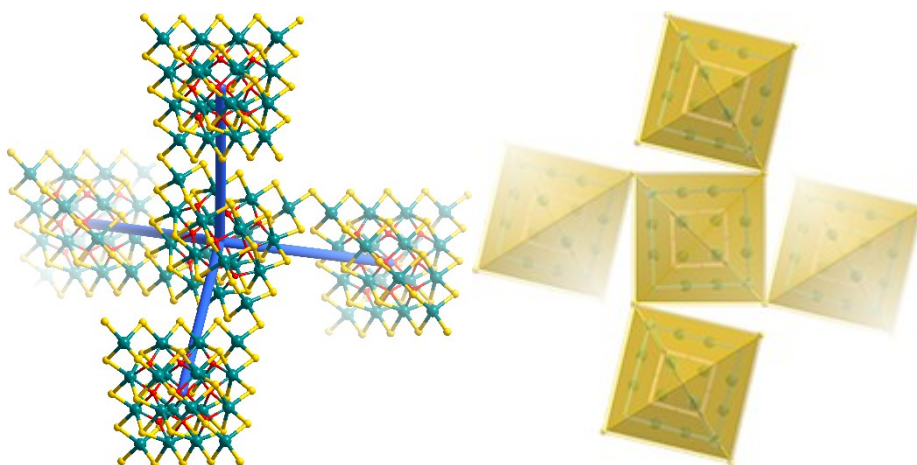


Fig. S2 Linkage mode between filled-T4 “[$\text{Sn}_{20}\text{O}_{10}\text{S}_{34}$]” clusters, each of which connects to four neighbors via four $\mu_2\text{-S}^{2-}$ -linkers of 3D-T4-SnOS.

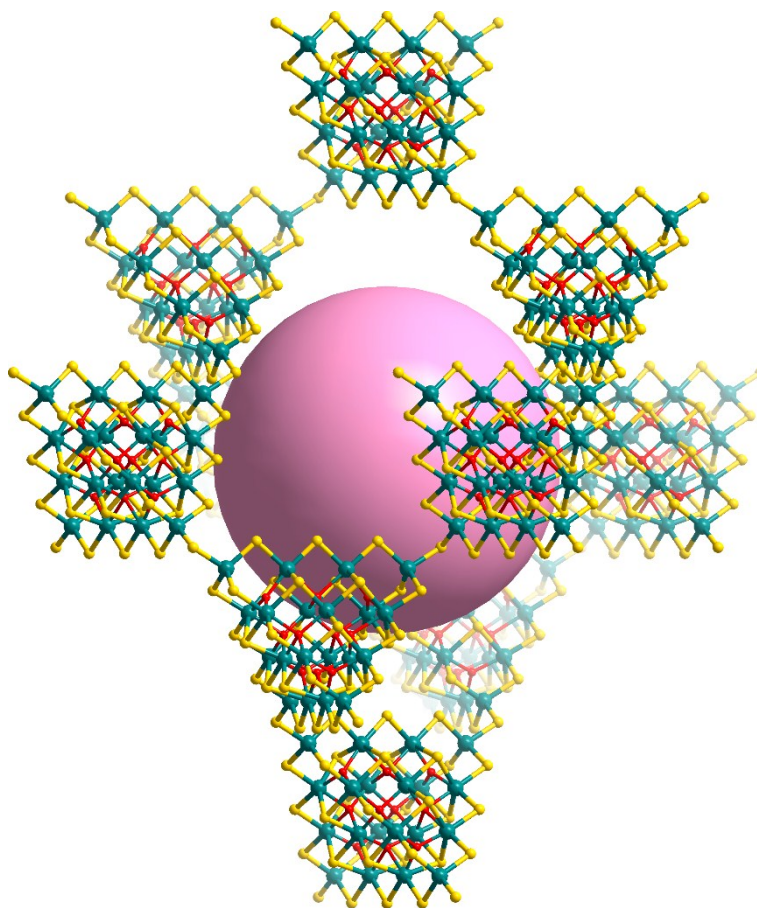


Fig. S3 Adamantane cage surrounded by 10 supertetrahedral filled-T4-“ $[\text{Sn}_{20}\text{O}_{10}\text{S}_{34}]$ ” clusters of 3D-T4-SnOS.

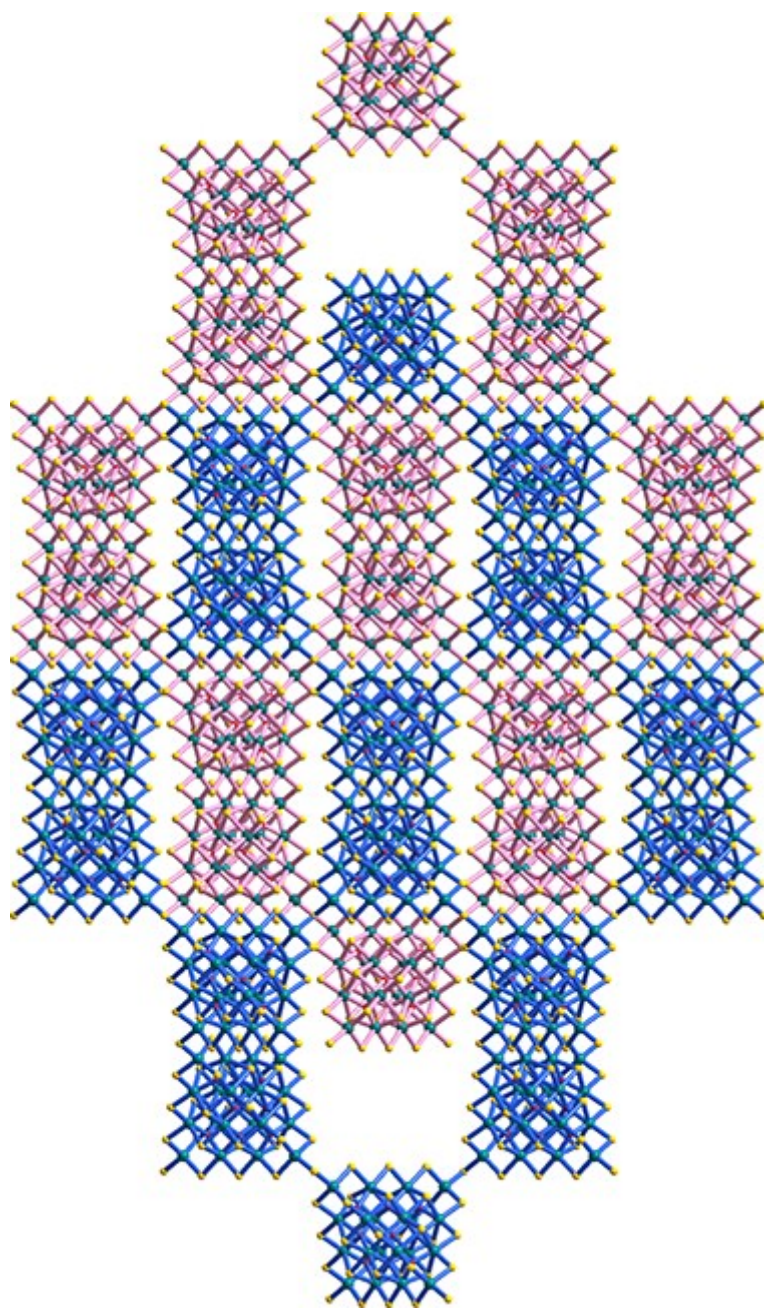


Fig. S4 Two-interpenetrated **dia**-typed framework of 3D-T4-SnOS in ball-stick fashion.

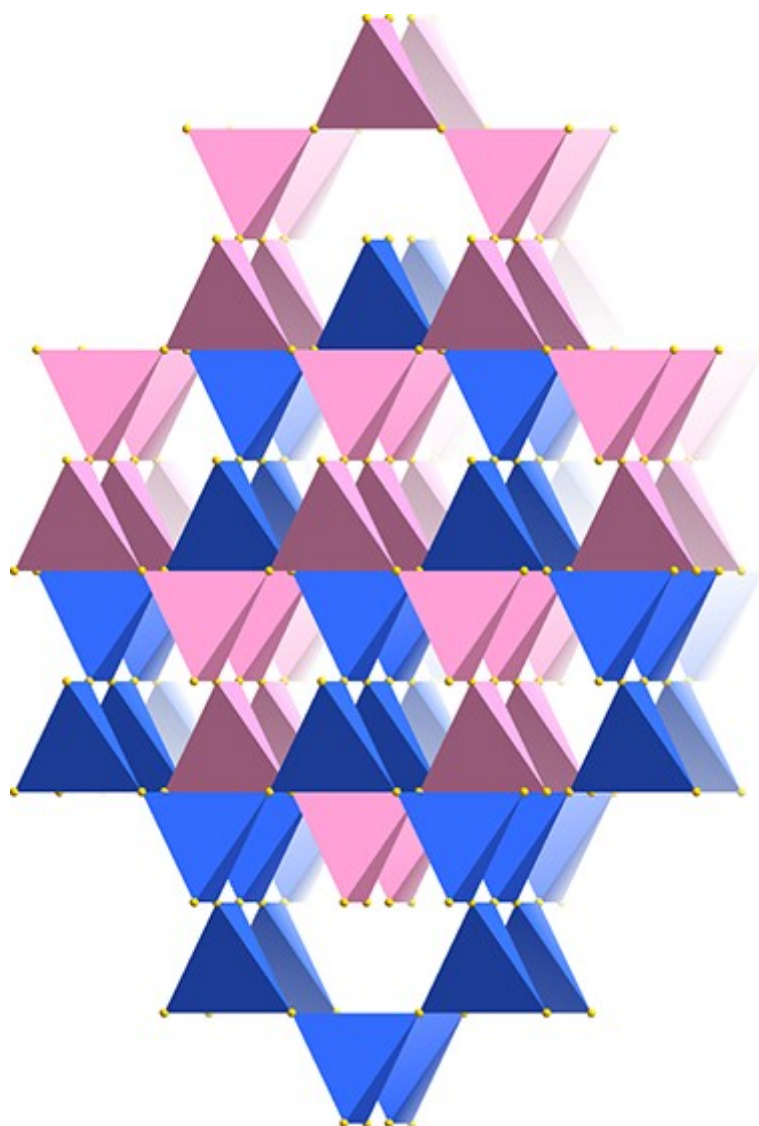


Fig. S5 Polyhedral scheme of two-interpenetrated **dia**-network of 3D-T4-SnOS.

Section S5: Powder X-ray Diffraction (PXRD)

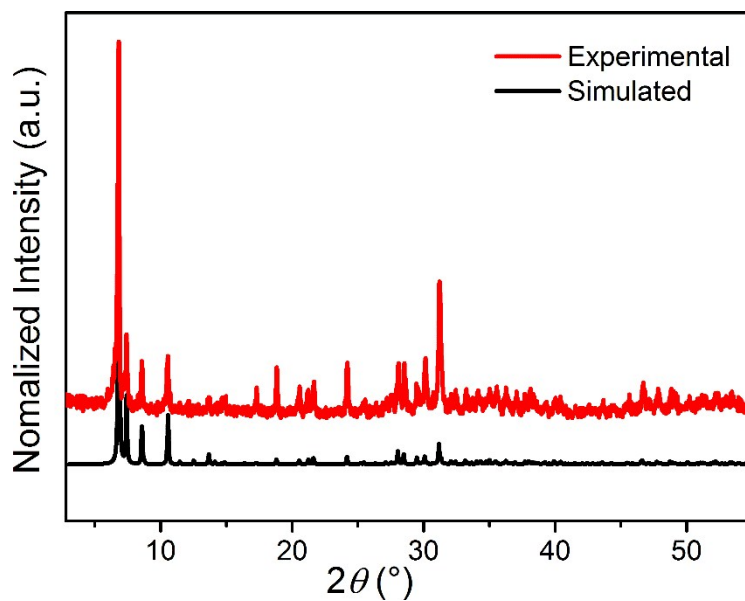


Fig. S6 Experimental and simulated PXRD patterns of 3D-T4-SnOS.

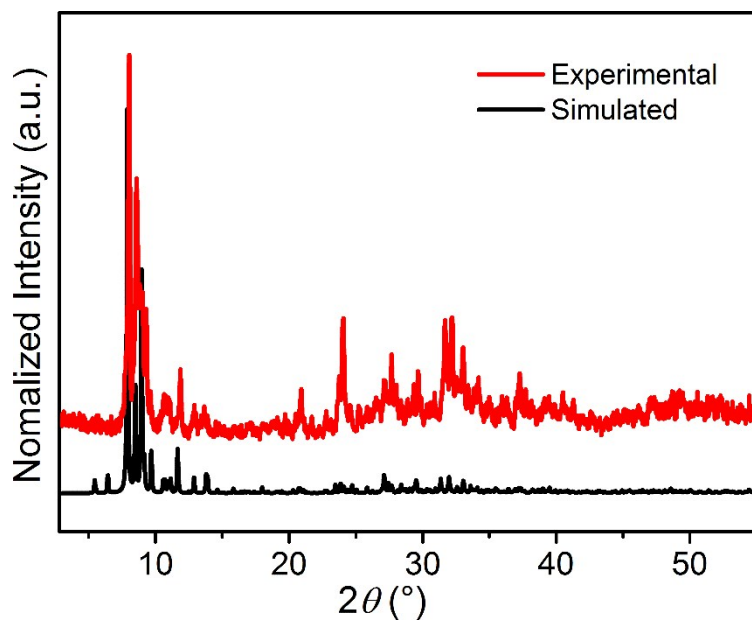


Fig. S7 Experimental and simulated PXRD patterns of 2D-T3-SnOS.

Section S6: Fourier-Transform Infrared Spectroscopy (FT-IR)

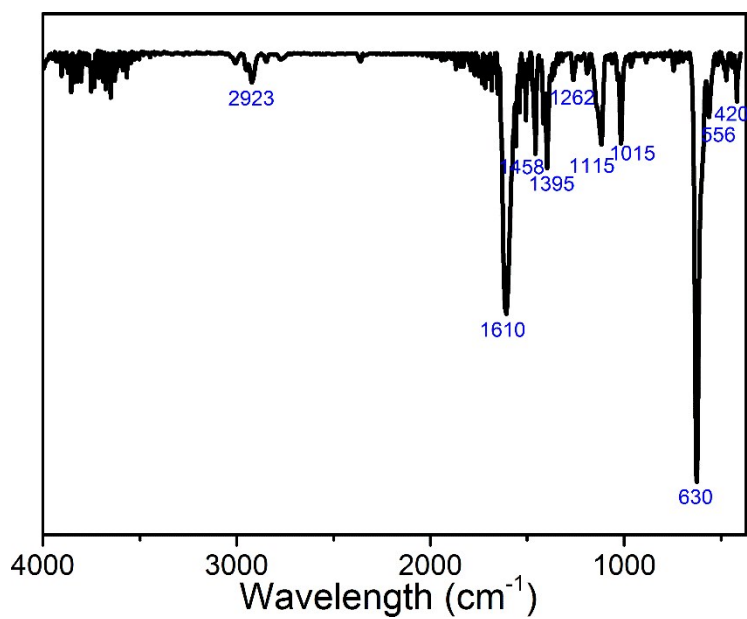


Fig. S8 FT-IR spectrum of 3D-T4-SnOS.

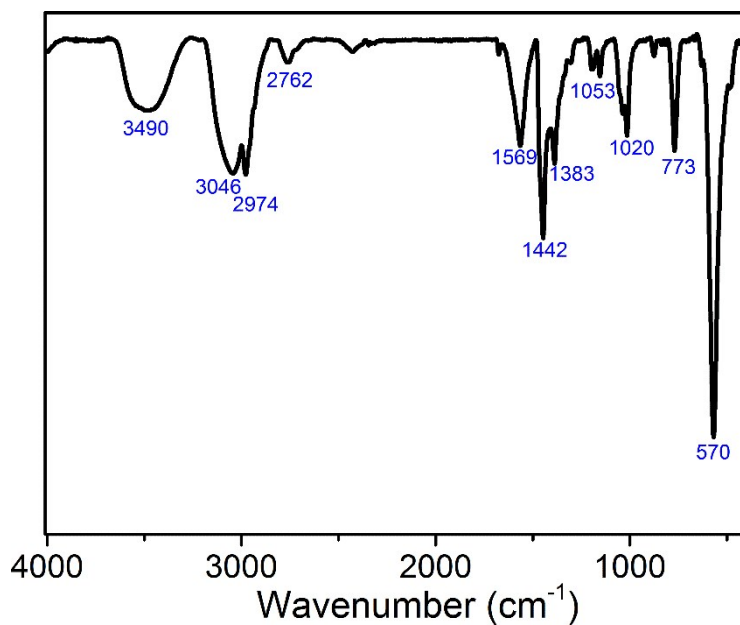


Fig. S9 FT-IR spectrum of 2D-T3-SnOS.

Section S7: Thermostability/Chemostability

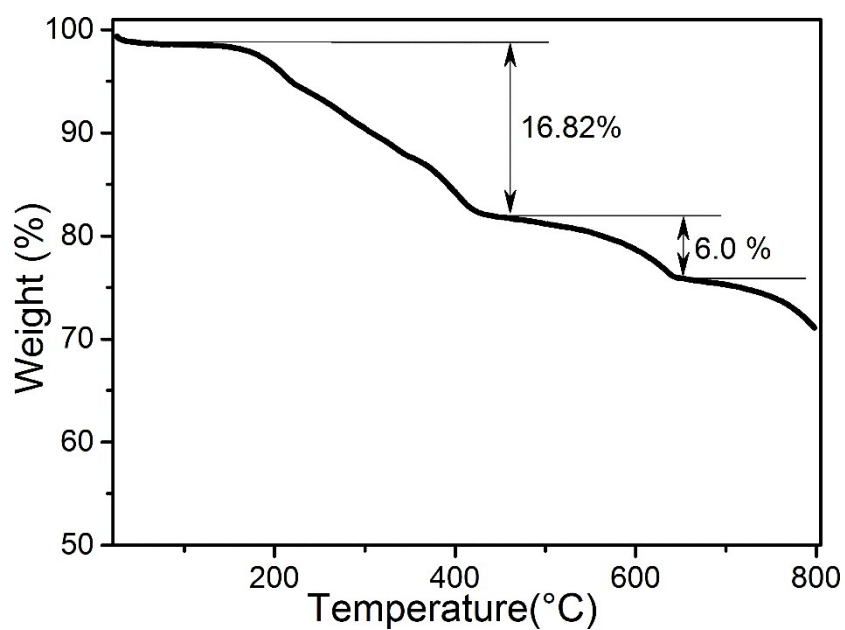


Fig. S10 TGA curve of 3D-T4-SnOS under N₂ atmosphere.

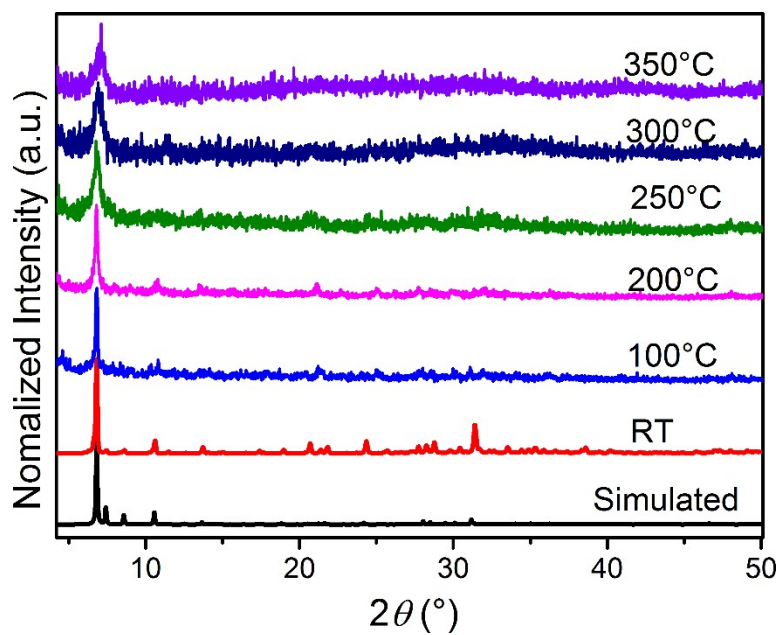


Fig. S11 Temperature-dependent PXRD patterns of 3D-T4-SnOS under N₂ atmosphere.

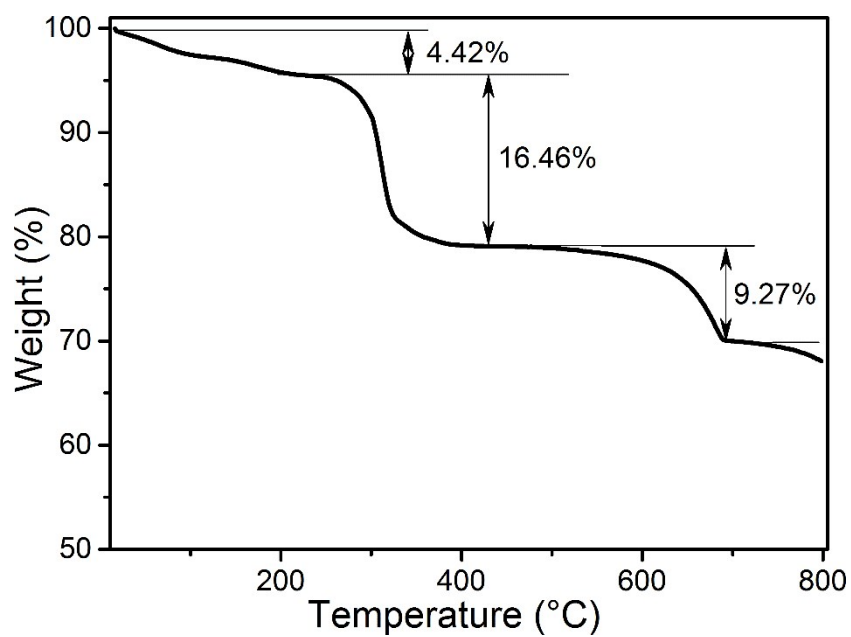


Fig. S12 TGA curve of 2D-T3-SnOS under N₂ atmosphere.

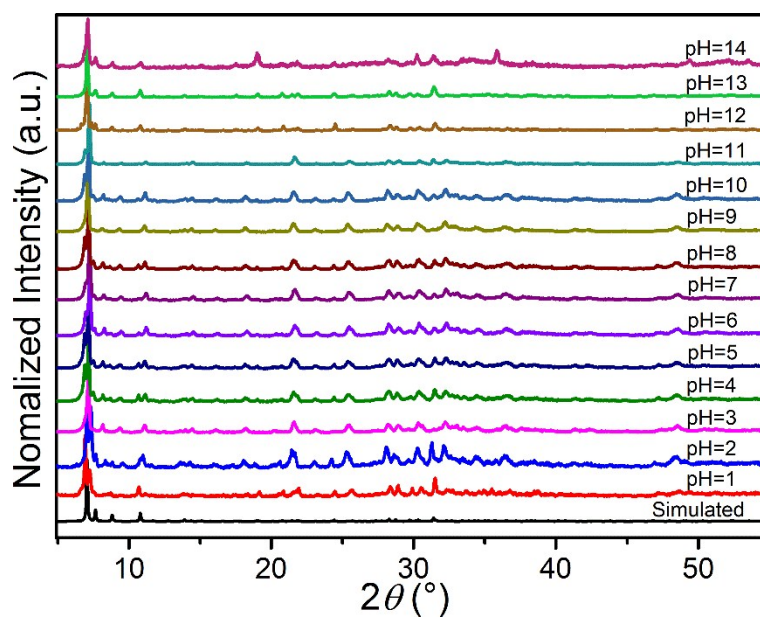


Fig. S13 PXRD patterns of 3D-T4-SnOS after immersion in aqueous solution with pH of 1~14 for 7 days.

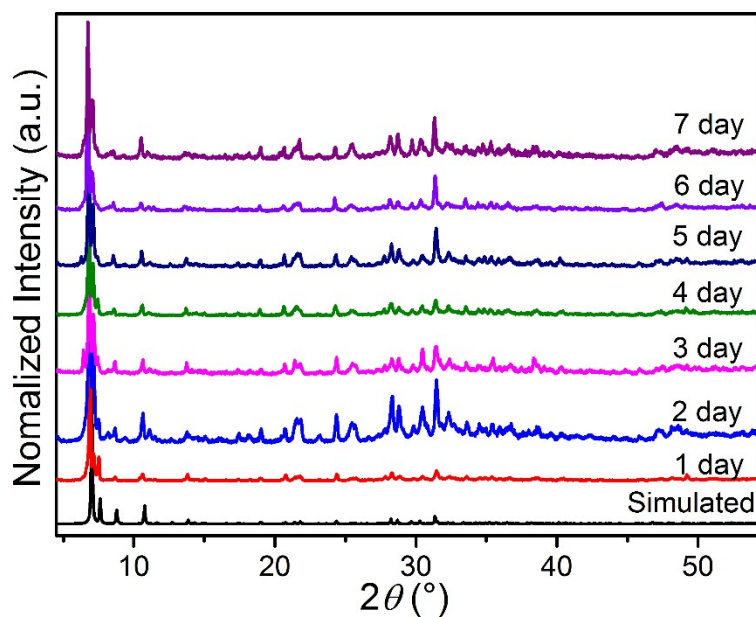


Fig. S14 PXRD patterns of 3D-T4-SnOS after immersion in pH = 1 aqueous solution for 1~7 days.

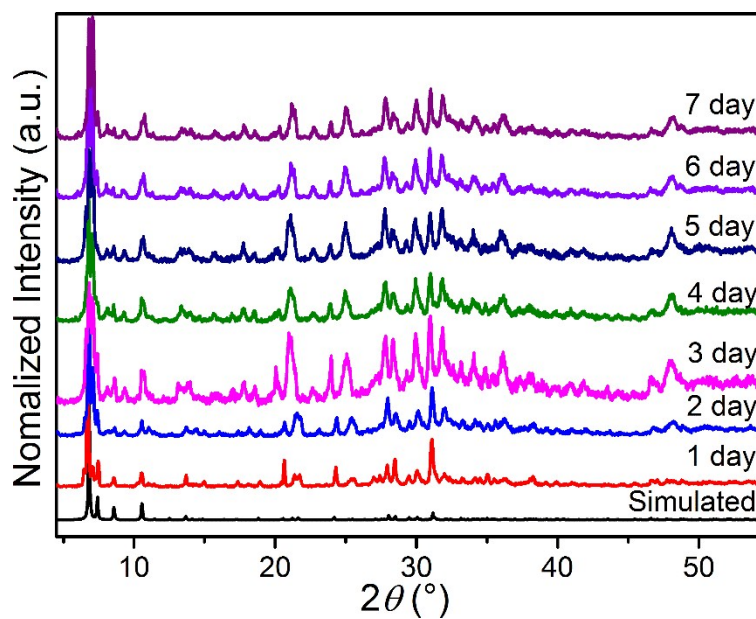


Fig. S15 PXRD patterns of 3D-T4-SnOS after immersion in pH = 2 aqueous solution for 1~7 days.

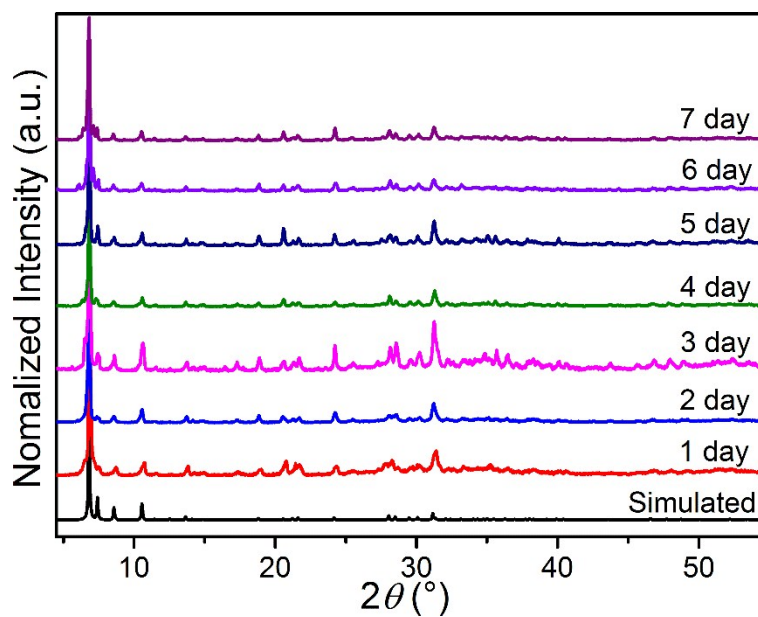


Fig. S16 PXRD patterns of 3D-T4-SnOS after immersion in pH = 12 aqueous solution for 1~7 days.

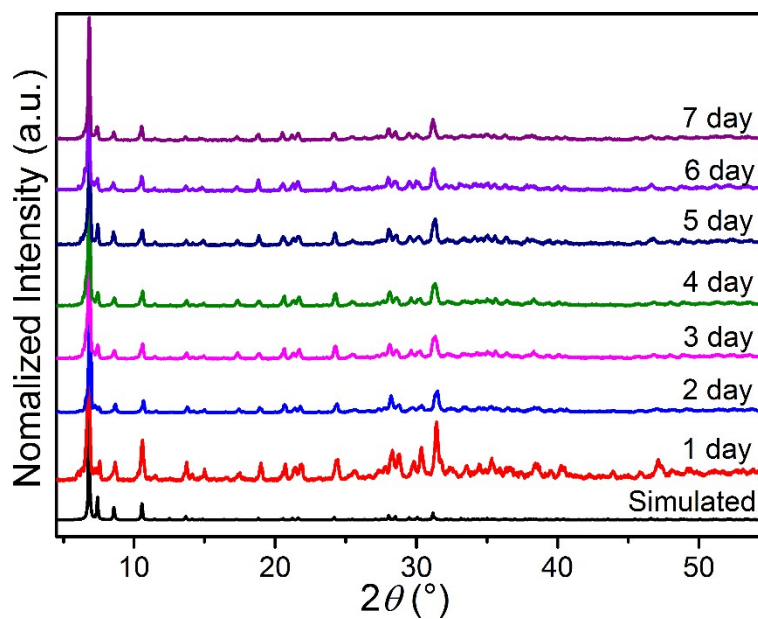


Fig. S17 PXRD patterns of 3D-T4-SnOS after immersion in pH = 13 aqueous solution for 1~7 days.

Section S8: Photoluminescence (PL)

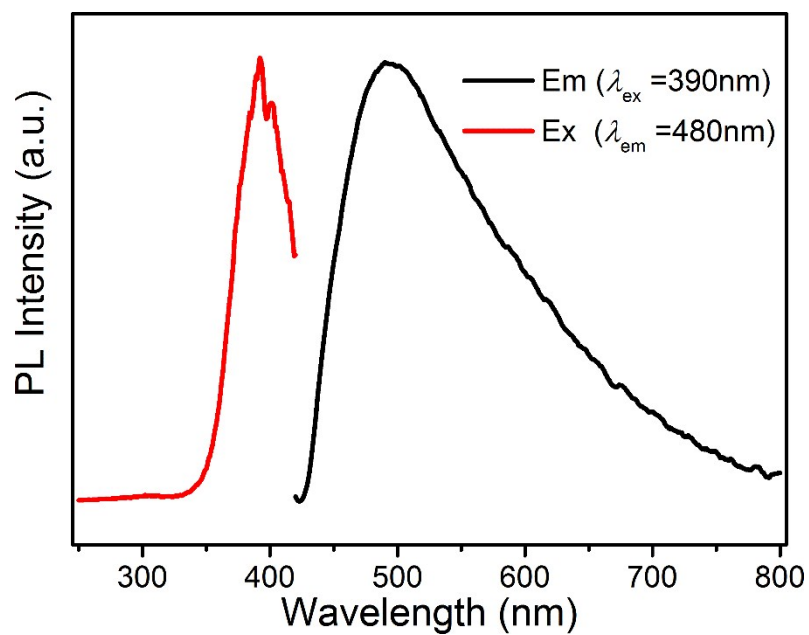


Fig. S18 PL excitation ($\lambda_{em} = 490$ nm) and emission ($\lambda_{ex} = 391$ nm) spectra of 3D-T4-SnOS at room temperature.

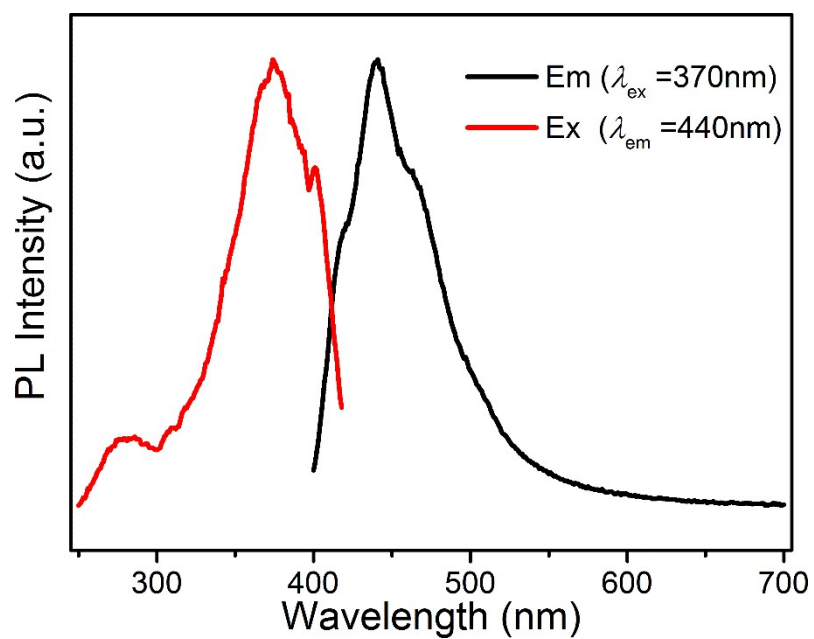


Fig. S19 PL excitation ($\lambda_{em} = 440$ nm) and emission ($\lambda_{ex} = 375$ nm) spectra of 2D-T3-SnOS at room temperature.

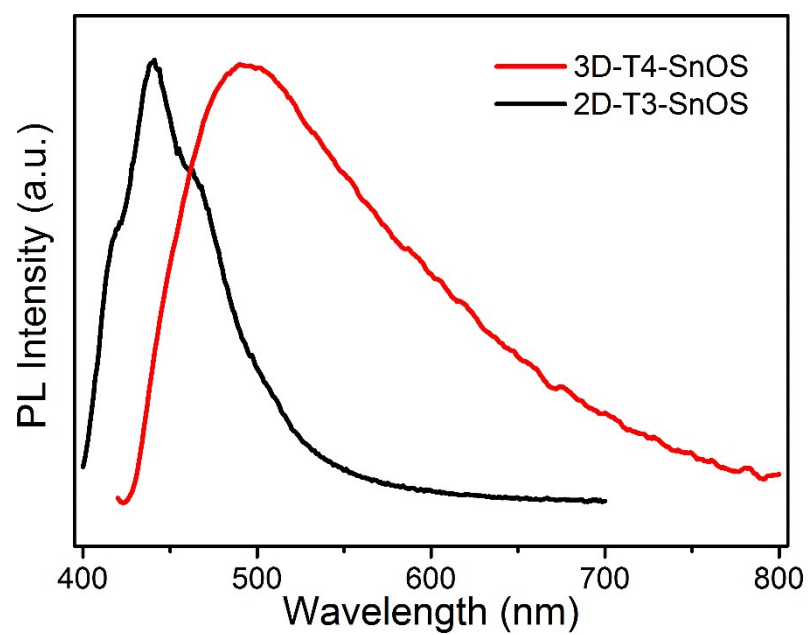


Fig. S20 PL emission spectra of 3D-T4-SnOS ($\lambda_{\text{ex}} = 391$ nm) and 2D-T3-SnOS ($\lambda_{\text{ex}} = 375$ nm) at room temperature.

Section S9: Photocatalytic degradation

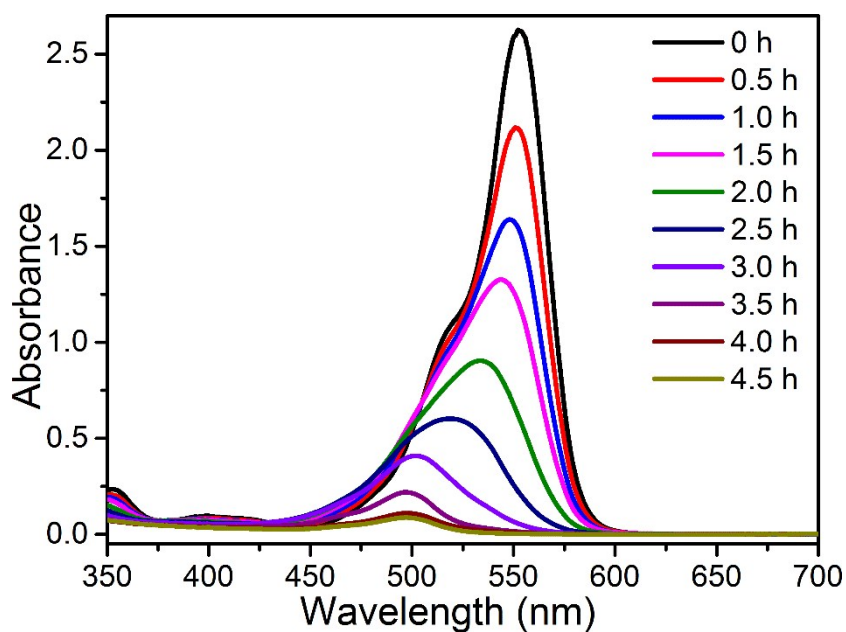


Fig. S21 UV-Vis absorption spectra during the photodegradation of rhodamine B in aqueous solution (pH = 7) over 3D-T4-SnOS under visible light irradiation.

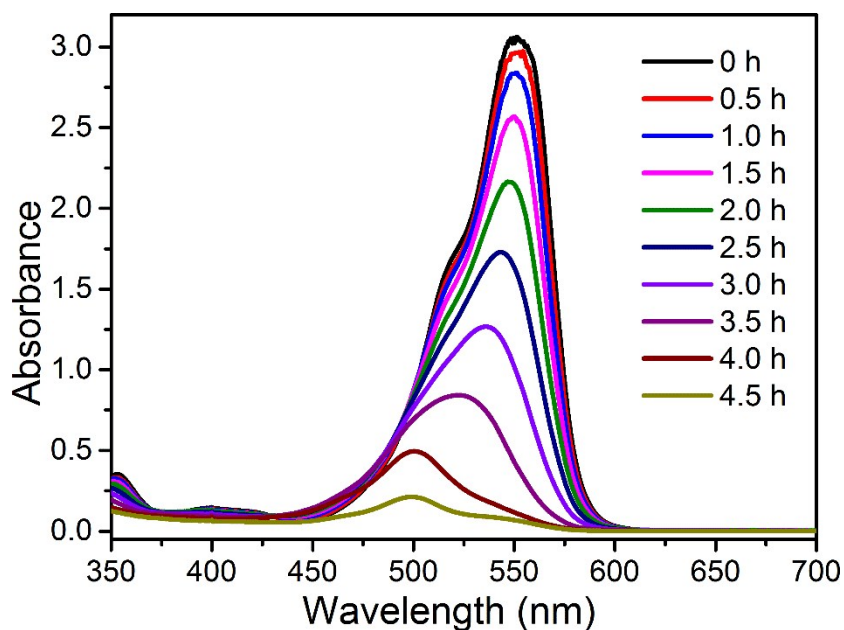


Fig. S22 UV-Vis absorption spectra during the photodegradation of rhodamine B in aqueous solution (pH = 5) over 3D-T4-SnOS under visible light irradiation.

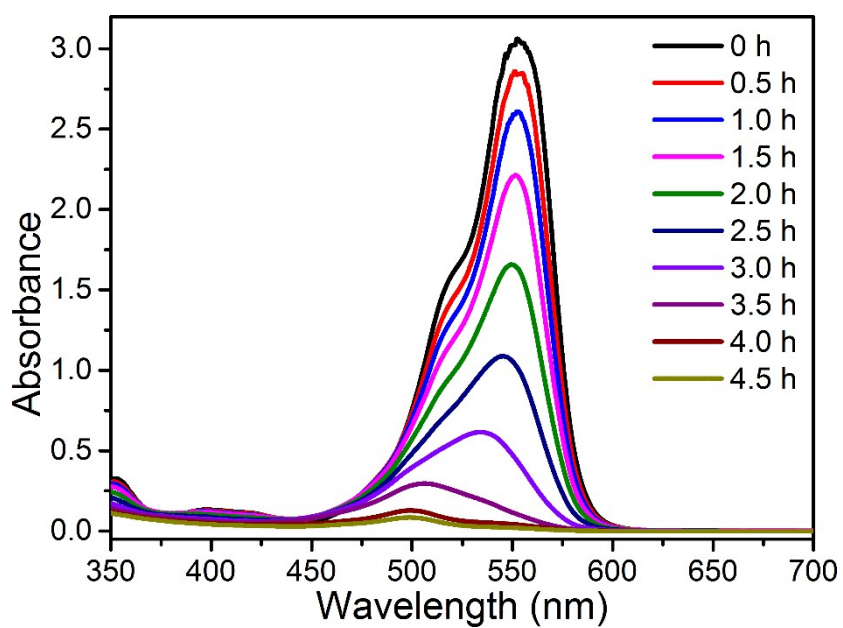


Fig. S23 UV-Vis absorption spectra during the photodegradation of rhodamine B in aqueous solution (pH = 3) over 3D-T4-SnOS under visible light irradiation.

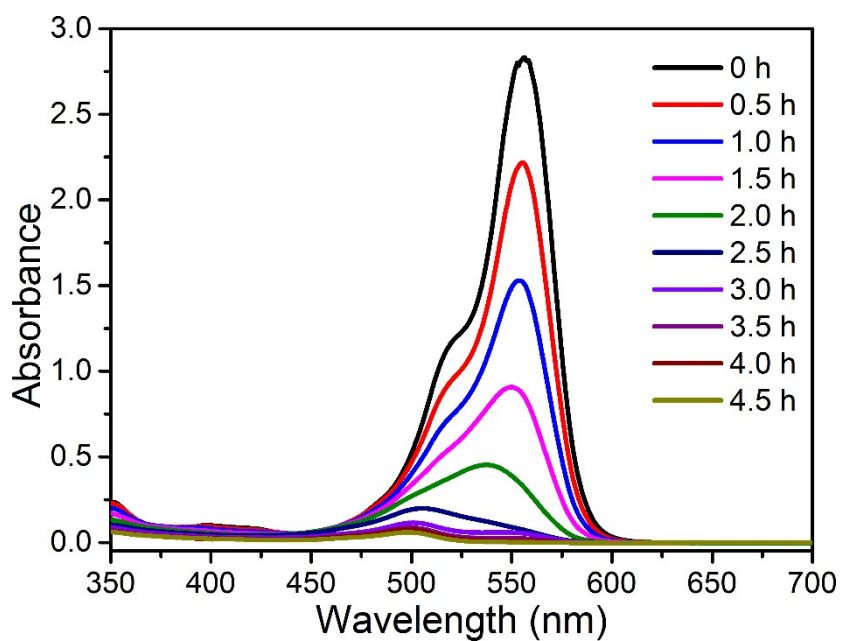


Fig. S24 UV-Vis absorption spectra during the photodegradation of rhodamine B in aqueous solution (pH = 2) over 3D-T4-SnOS under visible light irradiation.

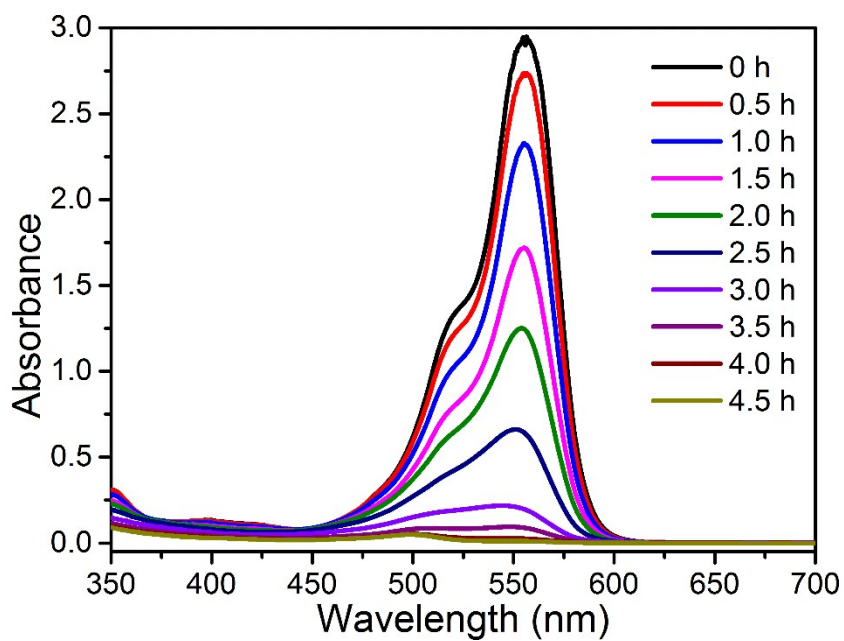


Fig. S25 UV-Vis absorption spectra during the photodegradation of rhodamine B in aqueous solution (pH = 1) over 3D-T4-SnOS under visible light irradiation.

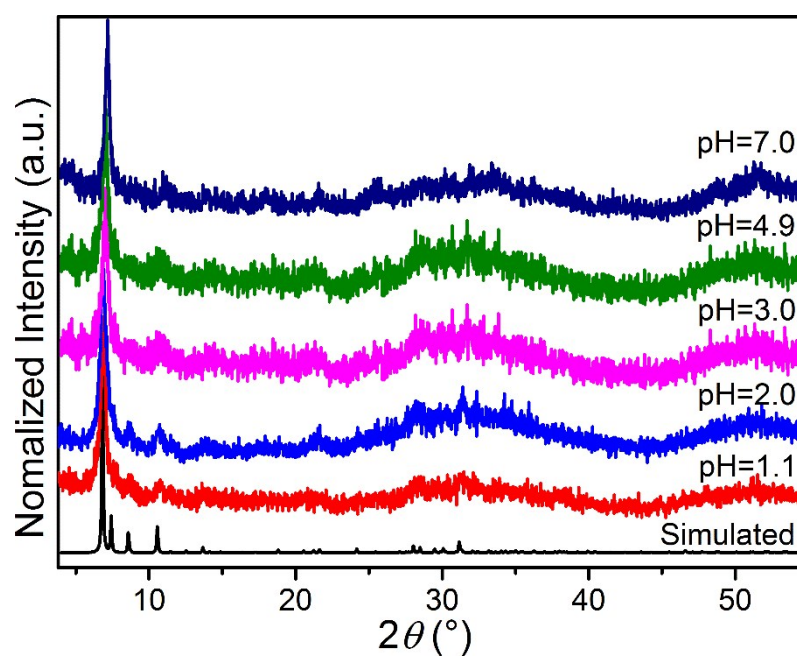


Fig. S26 PXRD patterns of 3D-T4-SnOS after photodegradation reactions.

Section S10: References

- [1] J. B. Parise, Y Ko, K. Tan, D. M. Nellis and S. Koch, *J. Solid State Chem.*, 1995, **117**, 219-228.
- [2] G. M. Sheldrick, Program for Crystal Structure Solution (University of Göttingen: Göttingen, Germany, 1997); SHELXT-Integrated Space-Group and Crystal-Structure Determination, *Acta Cryst.*, 2015, **A71**, 3-8; O. V. Dolomanov, L. J. Bourhis, R. J. Gildea, J. A. K. Howard and H. Puschmann, OLEX2: A complete structure solution, refinement and analysis program, *J. Appl. Cryst.*, 2009, **42**, 339-341.